Crowders Perturb the Entropy of RNA Energy Landscapes to Favor Folding

5 AUTHORS, INCLUDING:

Joon Ho Roh
United States Naval Research Laboratory
30 PUBLICATIONS **823** CITATIONS

SEE PROFILE

Reza Behrouzi
Harvard Medical School
12 PUBLICATIONS **95** CITATIONS

SEE PROFILE

Robert M Briber
University of Maryland, College Park
151 PUBLICATIONS **2,490** CITATIONS

SEE PROFILE

Crowders Perturb the Entropy of RNA Energy Landscapes to Favor Folding

Duncan Kilburn,[†] Joon Ho Roh,[†,‡,§] Reza Behrouzi,[†] Robert M. Briber,[*,‡] and Sarah A. Woodson[*,†]

[†]T. C. Jenkins Department of Biophysics, Johns Hopkins University, Baltimore, Maryland 21218, United States
[‡]Department of Materials Science and Engineering, University of Maryland, College Park, Maryland 20742, United States
[§]NIST Center for Neutron Scattering Research, National Institute of Standards and Technology, Gaithersburg, Maryland, United States

Ⓢ *Supporting Information*

ABSTRACT: Biological macromolecules have evolved to fold and operate in the crowded environment of the cell. We have shown previously that molecular crowding stabilizes folded RNA structures. Here we report SAXS measurements on a 64 kDa bacterial group I ribozyme in the presence of mono- and divalent ions and PEG crowders of different molecular weight. These experiments show that crowders always stabilize the folded RNA, but this stabilization is weaker in NaCl solutions than MgCl$_2$ solutions. Additionally, we find that RNAs with the same global structure, parametrized by R_g, have different scattering functions depending upon the ratio of electrostatic and entropic stabilization by ions and crowders, respectively. We quantify this difference using the scattering length per scattering volume and find that this ratio is larger for RNAs that fold in lower ionic strength solutions due to the higher crowder content. We conclude that lower RNA flexibility, or reduced configurational entropy, widens the free energy gap between the unfolded and folded RNA in crowded MgCl$_2$ solutions.
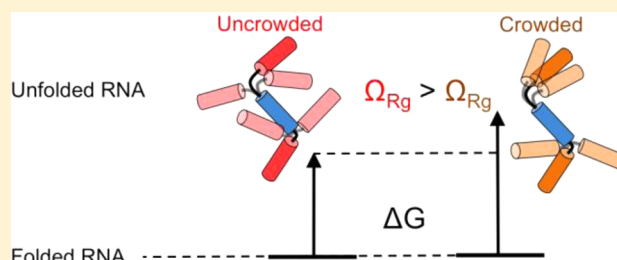
INTRODUCTION

Most RNA molecules must fold into a specific structure, or ensemble of structures, to fulfill their cellular functions such as enzymatic activity.[1] They have evolved to do this in a cellular environment that contains multiple species of ions and osmolytes and in which up to 30% of the volume is occupied by other macromolecules, or crowders.[2,3] We seek a more complete understanding of how a crowded environment affects RNA structure and folding.

The problem of folding an RNA molecule can be conceptually split into two distinct barriers to folding. First, the RNA must overcome electrostatic repulsion between the negatively charged phosphate groups on the RNA backbone. Models explaining how counterions reduce the backbone electrostatic repulsion and stabilize more compact, folded, RNA structures have become more complex over time, ranging from polyelectrolyte theory,[4] explicit handling of electric fields via solutions to the Poisson−Boltzmann equation,[5,6] to computationally expensive solutions to folding landscapes rendered using molecular dynamics (MD) simulations.[7] Second, the unfolded ensemble has more possible configurational states than the folded state, creating an entropic barrier to folding. Principles that explain how crowders modify the entropy of folding landscapes have been less extensively verified. Our experiments measure how macromolecular crowders alter the entropic states of folded and unfolded RNA and thus the transition between them. We anticipate that these insights from

model systems will be applicable to the crowded environment *in vivo*.

Other cellular molecules such as proteins and nucleic acids can interact with RNA and influence its folding landscape in a number of ways, most obviously through surface energies and electrostatic interactions. The occupation of volume by cosolutes (called crowders) can influence the chemistry of RNA molecules due to the excluded volume of the crowders.[8−13]

Excluded volume effects arise from interactions on the length scales of individual chains ("inter-molecular") and of chain segments ("intra-molecular"). Intermolecular crowding prevents the center of mass of a given particle from accessing certain regions in a solution, thus reducing its translational entropy and increasing its chemical potential. This depends on the overall size and shape of both types of particles.[2,9] Intramolecular excluded volume due to crowders is directly analogous to internal excluded volume that gives rise to self-avoiding walks for real polymer chains.[14] In this scenario, the crowders hinder certain configurations of the unfolded RNA but do not appreciably confine its center of mass. Therefore, the dominant effect is to reduce the internal configurational entropy of the RNA molecule. It should be noted that a

complete calculation of excluded volume includes contributions from both inter- and intra- molecular excluded volume.

Previous reports have reached conflicting conclusions about the effects of crowding. On the one hand, molecular crowders have been reported to stabilize the active states (and tertiary structures) of macromolecules. For example, self-cleavage and turnover of a 50 nucleotide hammerhead ribozyme is promoted by nonspecific macromolecules[15,16] and neutral crowding cosolutes, including polyethylene glycol (M_w = 8000).[17] Theoretical treatments have shown that crowded conditions favor specific compact conformers of RNA.[18,19] It was recently shown that the inert crowding agent Ficoll perturbs the unfolded state of a monomeric 18-kDa protein, making it more compact.[20]

On the other hand, small cosolutes (osmolytes) have been found to *destabilize* RNA secondary structure.[21] Other studies have similarly measured a destabilizing effect of protein crowding on the stability of folded proteins,[22] which the authors attribute to destabilizing nonspecific interactions with other protein molecules. Thus, the many interactions that drive protein and nucleic acid folding in the cell are extremely difficult to disentangle.[23] We used synthetic polymers to specifically perturb the entropy of the RNA's folding landscape, while acknowledging that this is but one of many competing forces that affect folding *in vivo*.

Here, we present results that demonstrate two interconnected phenomena of how crowders alter RNA folding. First, crowders shift the folding transition of the Azoarcus ribozyme to lower salt concentrations. We reported this previously for PEG1000 in $MgCl_2$ solutions,[24] but now we demonstrate this for higher molecular weight crowders, and for NaCl solutions. Second, we show that the unfolded RNA structure depends on the types of crowder and ions in the solution, even for RNAs with identical radii of gyration. For $MgCl_2$ or NaCl, lower bulk ionic strength solutions generally result in stiffer RNAs with fewer possible configurations. We postulate that these differences are due to different contributions to RNA stability from electrostatic and entropic effects, and that these differences play an important role in the observed stabilization of the folded RNA.

■ EXPERIMENTAL METHODS AND MATERIALS

RNA Preparation. The *Azoarcus* ribozyme (195 nt) was transcribed *in vitro* from pAz-IVS digested with *Ear*I and gel purified as described previously.[25,26] The stock was incubated at 50 °C for 5 min before use. RNA solutions for SAXS experiments were 0.4 mg/mL in 20 mM Tris-HCl (pH 7.5) with the desired PEG concentration. Prior to each measurement, the RNA solution was incubated for 5 min at 50 °C and then 30 min at 37 °C. The unfolded and folded radiuses of gyration, R_gs, were also measured separately from metal ion titrations; these samples were prepared by diluting from the same RNA stock solution to minimize error.

SAXS. SAXS measurements were performed using: BioCAT (18ID) at Argonne National Lab Advanced Photon Source; SIBYLS (12.3.1) at the Advanced Light Source, Lawrence Berkeley National Lab; and X9 at the National Synchrotron Light Source, Brookhaven National Lab. The wavelength was 1.033 Å (energy 12 keV) and measurements were made in the momentum transfer range 0.006–0.34 Å^{-1}. SAXS data were radially averaged and corrected for background signal due to the buffer. We checked that radiation damage was minimized for all measurements.

PEG has intrinsically low X-ray contrast with water (0.56 mols of electrons per cm^3) allowing the measurement of RNA structure (approximately 0.93 mols of electrons per cm^3) without significant interference from the PEG. Higher sample flow rates were used for the

samples with higher M_w PEG as we found that the X-rays caused the PEG to accumulate on the capillary walls, leading to perturbed scattering functions indicative of molecular aggregates. Lowering the X-ray dose per molecule by increasing the sample flow rate removed this artifact.

Guinier analysis of the SAXS data gives us two fitted parameters: the radius of gyration of the RNA, R_g, and the extrapolated scattering intensity at $Q = 0$, I_0. We used I_0 to calculate the correlation length per scattering volume (see Results section) at a given R_g. The Guinier-defined R_gs are consistently lower than the R_gs from real-space analysis for the unfolded RNA. There is no discrepancy for the folded RNA. With this difference accounted for, the data match those published previously for the PEG1000 series.[24]

2-State Model for RNA Folding. Owing to its cooperativity, RNA folding is commonly approximated by a 2-state model[27−29] which can adequately describe the folding thermodynamics of small hairpins[30,31] and large RNAs for which the intermediate structures represent a small fraction of the occupied RNA states, such as the *Azoarcus* ribozyme.[26,32] Since the measured R_g is an order parameter of the solution that reflects the average population of folded and unfolded RNA, the change in R_g with increasing $MgCl_2$ or NaCl concentration was fit to modified Hill equations:

$$R_c^2 = (R_{U,0} - kc)^2 - \frac{c^n}{c_m^n + c^n}[(R_{U,0} - kc)^2 - R_F^2] \tag{1}$$

$$R_c^2 = (R_{U,0} - k\log(c))^2 - \frac{c^n}{c_m^n + c^n}[(R_{U,0} - k\log(c))^2 - R_F^2] \tag{2}$$

in which R_c is the radius of gyration at Mg^{2+} concentration c, $R_{U,0}$ is the radius of gyration of the unfolded RNA at zero $MgCl_2$, k is dR_g/dc above the folding transition in eq 1 and $c\ln(10)\,dR_g/dc$ in eq 2, c_m is the folding midpoint concentration, R_F is the radius of gyration of the folded RNA, and n is the Hill coefficient. Equation 2 was used for the NaCl titrations because the $(R_{U,0} - kc)$ term was insufficiently constrained by our data above c_m. The linear decrease in R_g with c (or $\log(c)$) before the folding transition accounts empirically for a contraction of the unfolded ensemble with Mg^{2+} or Na^+.[33]

As the Mg^{2+} (or Na^+) is increased, preferential interaction of the ions with the folded RNA versus the unfolded RNA shifts the folding equilibrium toward the folded state.[34] This cooperativity of folding with respect to Mg^{2+} concentration is recapitulated by mean field theories[5,35] or discrete models[36] of the ion-RNA interactions for small RNAs. As noted by Leipply and Draper,[37] this slope corresponds to the preferential ion interaction coefficient in systems with constant co-ion activity coefficients (see Discussion below). Although the empirical relationship in eqs 1 and 2 does not provide information about the microscopic ion-RNA interactions, it allows us to compare the experimental folding free energy at different ion and crowder concentrations.

■ RESULTS AND DISCUSSION

Molecular Crowding by PEG. We used PEG as the crowder molecules for a number of reasons. First, PEG is very useful for SAXS studies as it has a very low electron density contrast with water and so we can extract the scattering function of the RNA with little cross-particle scattering intensity. Second, it is anticipated that PEG has relatively low surface interactions with RNA, extrapolating from the modest surface effects of the ethylene glycol monomer demonstrated by Lambert and Draper.[21]

The volume excluded by a crowder depends on the average M_w and number density of the particles. A further complication is that PEG itself undergoes a transition between dilute and semidilute thermodynamic states in the range of concentrations that we are interested in. Below the crossover concentration, $C^{\#}$, the crowders behave as independent particles with little

direct interaction. At $C^{\#}$, the PEG molecules start to interpenetrate, eventually forming a network. Using equations of states that explicitly incorporate $C^{\#}$ to describe changes to the concentration dependence of osmotic pressure, $C^{\#}$ can be established for PEG in water, a good solvent.[38] By this empirical determination, $C^{\#}$ is found to be 17.6% for PEG1000, 6.7% for PEG3350 and 3.3% for PEG8000.

PEG Compresses Unfolded and Folded RNA. We first asked to what degree the structures of the folded and unfolded RNA depend on the volume available in the solution. Figure 1a shows a decrease in the R_g of the unfolded RNA with increasing crowder content, in PEG solutions containing 20 mM Tris-HCl pH = 7.5 but no added Mg^{2+}. We assume that the R_gs of the unfolded (U) state represent a population of RNA molecules
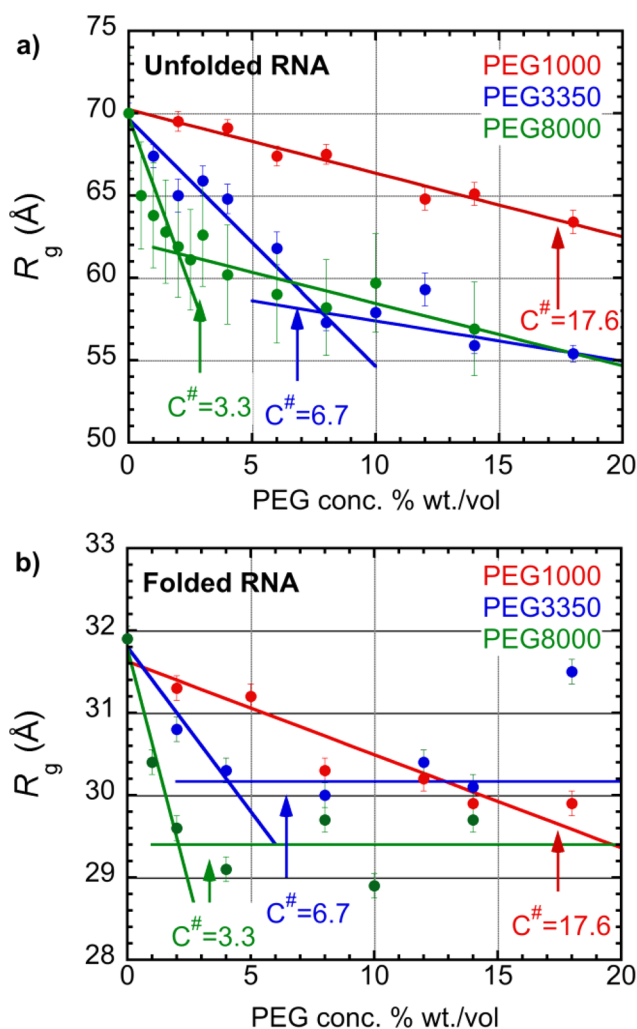

Figure 1. Crowders favor smaller RNA structures. Radius of gyration (R_g) of the *Azoarcus* ribozyme as a function of crowder (PEG) concentration. (a) Unfolded RNA (0.4 mg/mL) in 20 mM Tris-HCl, pH 7.5. (b) Folded RNA (0.4 mg/mL) in Tris buffer plus 2 mM $MgCl_2$. The crossover concentrations, $C^{\#}$, mark the transition from dilute ($C < C^{\#}$) to semidilute ($C > C^{\#}$) PEG solutions. The error bars represent 1 s.d. Data above and below the crossover concentrations were fit to a line (least-squares), omitting the point at 18% PEG3350 which deviates from this trend. The fitted lines are extrapolated beyond the crossover concentrations to emphasize the different behavior above and below $C^{\#}$. These fits are intended to guide the eye. This range of PEG concentrations is too narrow to discriminate among theoretical models of crowded solutions.[10]

with a distribution of R_gs rather than a single 'unfolded' structure. Thus, higher concentrations of PEG shift the unfolded population to structures with lower average R_g values.

In PEG1000, R_g(U) decreases linearly with increasing PEG over the range tested (Figure 1a). The smaller R_gs observed in more crowded solutions are to be expected as the excluded volume effect *per se* always favors smaller structures. The PEG1000 data are all in the dilute regime (the highest concentration, 18% is just above the crossover concentration, $C^{\#}$ of 17.6%). PEG3350 and PEG8000 cause a steeper decrease in R_g than PEG1000 does, below their crossover concentrations $C^{\#}$ of 6.7% and 3.3%, respectively. This trend diminishes in semidilute solutions of PEG3350 and PEG8000 (Figure 1a), to the degree that the R_gs in 18% PEG3350 and 18% PEG8000 are the same (56 Å). We hypothesize these trends converge because at these concentrations, the solutions form networks of PEG with the result that the PEG molecules lose their independence. Thus, the crowding effect above $C^{\#}$ becomes a function of the network size[39] which depends upon the overall PEG concentration and not on the molecular weights of the chains. Alternatively, the R_g of the RNA has reached a minimum value prior to the folding transition.

Recently, Sugimoto et al. concluded that excluded volume effects were not the major reason for an increase in a 58 nt hammerhead ribozyme's activity in crowded solutions.[16] They reasoned that the ribozyme activity increased in PEG8000 because the crowder simultaneously destabilized the RNA secondary structure and stabilized its tertiary structure. A similar effect was recorded for DNA duplexes (secondary structure),[40] and higher-order DNA structures such as quadruplexes[41] or three-way junctions.[42] These conclusions are in agreement with those of Lambert and Draper on the effects of ethylene glycol on a range of RNAs,[21] which were taken to be dominated by interactions between ethylene glycol and the RNA surface.

Our results cannot be explained by destabilization of the RNA secondary structure, however. In a previous study, the R_g of the unfolded *Azoarcus* ribozyme increased from 60.5 to 67.5 Å (1 mg/mL RNA) when the secondary (and tertiary) interactions were diminished by 3 M urea.[43] By contrast, Figure 1 shows a *decrease* in the unfolded RNA's R_g with increasing crowder content, indicating that the destabilization of secondary structure is not the dominant effect of PEG.

Additionally, we measured titrations with ethylene-glycol (EG) as cosolute (Figure S1e, Supporting Information). EG has a much larger surface area and also perturbs the water activity more than PEG for a given wt./vol. concentration. Thus any surface- or solvation-driven effects are expected to be maximized in EG. It has been shown in a similar nucleic acid system that EG lies on the continuum of PEG behavior,[44] so subtle differences in surface chemistry are negligible. In contrast to the PEG measurements, the R_g of the unfolded RNA *increases* in EG. Thus, excluded volume or entropic effects stabilize more compact structures and are bigger in magnitude than the destabilizing effects on the secondary structure.

PEG also reduces the size of the folded RNA in 2 mM $MgCl_2$, which is shown in Figure 1b. This observation suggests that the crowders stabilize smaller structures than those achieved through electrostatic forces alone, and further implies that the ribozyme is not optimally packed at 37 °C.

We separately measured the native state occupancy of the ribozyme using an RNA cleavage reaction, and observed that PEG does indeed increase the ribozyme's activity, particularly at

MgCl$_2$ in the range 0.8 to 1.1 mM (R. Desai and D.K., data not published). Therefore, PEG does not obstruct the ribozyme active site and appears to stabilize the true native state.

PEG Stabilizes Folded RNA in MgCl$_2$ and NaCl. We next investigated how crowding changes the stability of the folded state with respect to the unfolded ribozyme. We previously showed that the *Azoarcus* ribozyme folds cooperatively in MgCl$_2$, and that the free energy difference of the folded and unfolded states can be extracted from the change in R_g.[25]

We remeasured the scattering functions of the *Azoarcus* ribozyme in MgCl$_2$ and PEG1000 solutions, with finer sampling in the transition region to define the transition midpoint with lower error (see Supporting Information Figure S1a). To determine whether excluded volume effects depend on the counterion used to fold the RNA, we also titrated the ribozyme with NaCl in various amounts of PEG1000 (Figure S1b, Supporting Information). Finally, we compared the effect of crowder size by repeating the experiments in PEG with a molecular weight of 3350 Da (Figure 2) or 8000 Da (Figure S1c,d, Supporting Information). In each case, the midpoints of the transitions are shifted toward lower MgCl$_2$ and NaCl concentrations with increasing crowder concentration, demonstrating that the crowder stabilizes the folded form of the ribozyme as previously observed.[24]

The parameters from the fits to eqs 1 and 2 are shown in Table S1 for the MgCl$_2$ titrations and Table S2 for the NaCl titrations (see Supporting Information). The midpoint of the folding transition, c_m, decreases monotonically with increasing PEG, and this trend is identical for PEG1000 and 3350 (Figure 2 and Figure S1, Supporting Information). PEG8000 stabilizes the folded RNA more than PEG1000 or PEG3350 at low crowder concentrations, but the decrease in c_m saturates around 8−10% (Figure S1, Supporting Information). The steepness of the transitions, n, appears constant with respect to both PEG concentration and M_w. The slope $n \approx 5.0 \pm 0.1$ for MgCl$_2$ and 1−1.5 for NaCl, consistent with our previous results.[33]

Draper and co-workers recently specified conditions in which n is roughly equivalent to the excess Mg^{2+} ions that stabilize the folded RNA, Γ_{2+}, including those ions that form long-range electrostatic interactions with the RNA.[37] The first condition is that the activity coefficient of Mg^{2+} ions remains constant in the range that is being evaluated; a method of achieving this is by having excess Cl$^-$ ions. They suggest a 30-fold excess of monovalent salt KCl. Our experiments are performed in 20 mM Tris-HCl, pH 7.5 which we calculate contributes a 27-fold excess of Cl$^-$ ions at 0.6 mM MgCl$_2$, approximately the midpoint of the 0% PEG transition. In our NaCl titrations, the activity coefficient of the cation changes more slowly than for MgCl$_2$.

The second condition is that Γ_{2+} be constant in the MgCl$_2$ range evaluated; we have no independent verification of this in our case, but the observation that n is constant for fits to all our data provides a *posthoc* justification for assuming it to be the case. A constant value of n indicates that the number of Mg^{2+} ions required to stabilize the folded RNA is independent of the crowder content. This is an important observation as it suggests an intrinsic role for ions in stabilizing the folded RNA, and raises the question: could the folded RNA be stabilized by crowders alone? As explained below, our results suggest not.

Change in Folding Free Energy. The decrease in c_m with increasing PEG is a reflection of the predicted stabilization of folded RNA by the crowders, and the values are consistent, within error, with our previously published data.[24] This
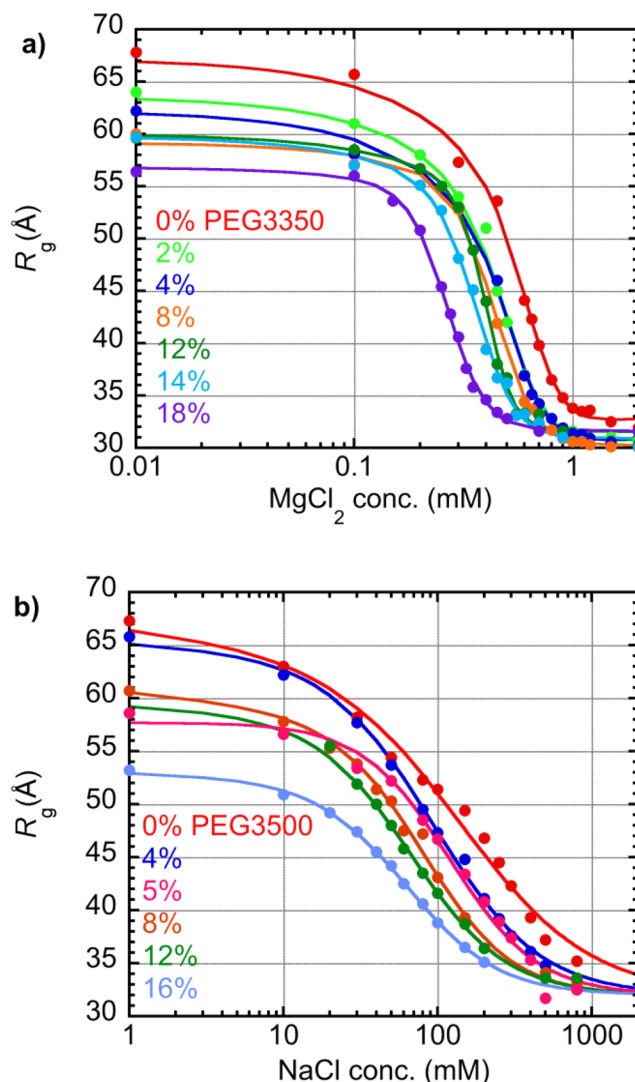

Figure 2. PEG stabilizes folded RNA at low cation concentrations. MgCl$_2$ and NaCl titrations showing the decrease in R_g of the *Azoarcus* ribozyme at 37 °C at a range of PEG 3350 concentrations. (a) Folding in MgCl$_2$. Solid lines are fits to an adjusted Hill equation (eq 1) assuming a two-state collapse and a linear decrease in R_g of the unfolded RNA with increasing MgCl$_2$ concentration. Parameters of the fits are given in Table S1, Supporting Information. Ionic strength is given by 2.5 × [MgCl$_2$]. (b) Folding in NaCl. Solid lines are fits to eq 2, which assumes R_g of the unfolded RNA is proportional to the logarithm of salt concentration. Parameters of the fits are given in Table S2, Supporting Information. Ionic strengths are equal to the molar concentrations. Typical values for 1 s.d. are ±1 Å for unfolded RNA and ±0.15 Å for folded RNA.

stabilization can be expressed as the difference between the free energy of folding in crowded solution and that in aqueous solution, $\Delta\Delta G = \Delta G_C - \Delta G_0$. To calculate this we consider folding at the midpoint in a crowded solution, $c_{m,C}$, at which $\Delta G_C = 0$. Following previous authors[27,28] we use the empirical fits in eq 1 and 2 to extrapolate ΔG_0 from $c_{m,0}$ where $\Delta G_0 = 0$ to $c_{m,C}$. We calculate the difference in the RNA's folding free energy between the aqueous and PEG-containing solution according to:

$$\Delta\Delta G = -nRT \ln \frac{c_{m,0}}{c_{m,c}} \quad (3)$$

where $c_{m,0}$ and $c_{m,c}$ are the MgCl$_2$ or NaCl concentrations at the folding midpoints in aqueous and crowded solutions, respectively, and n is the Hill coefficient.

PEG substantially stabilizes the folded RNA in MgCl$_2$, with $\Delta\Delta G$ reaching -4.3 ± 0.3 RT (-2.6 ± 0.2 kcal/mol at 37 °C) at 18% PEG (calculated from the average of PEG1000 and PEG3350; Figure 3a). To put these values in context, at 0.31
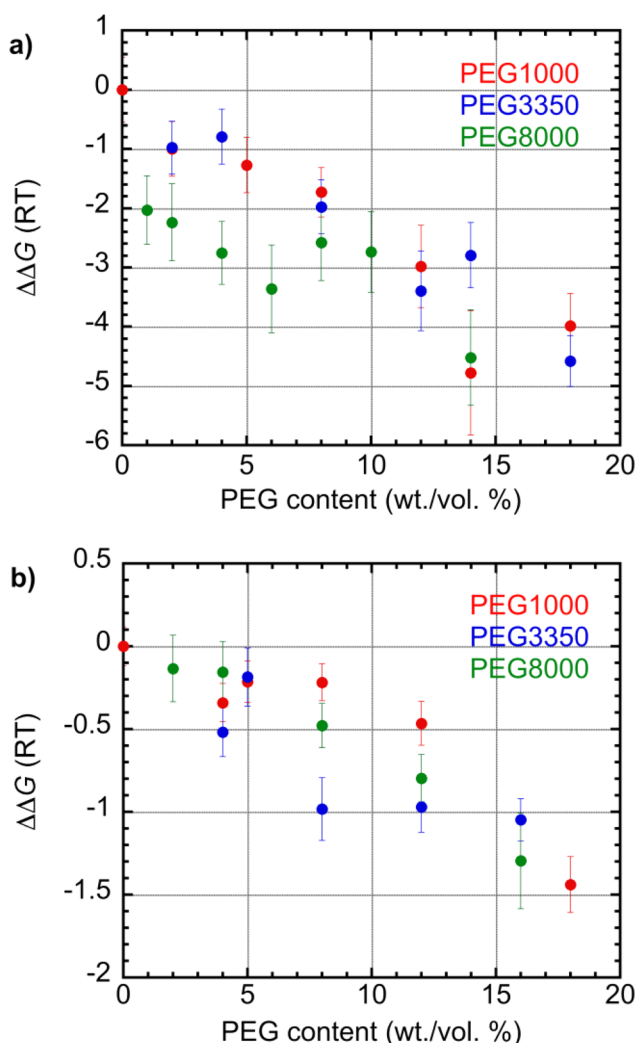

Figure 3. Folding free energy of *Azoarcus* ribozyme is decreased by crowding. $\Delta\Delta G$ is the change in ΔG of folding due to the presence of PEG as macromolecular crowders, with (a) MgCl$_2$ and (b) NaCl as the stabilizing counterion. Values were calculated using eq 3 and parameters from the fits of the Hill equation to experimental data. The data and fits for the MgCl$_2$ titrations are shown in Figure 2a, PEG3350; Figure S1a, PEG1000; Figure S1c, PEG8000, Supporting Information. The data and fits for the NaCl titrations are shown in Figure 2b, PEG3350; Figure S1b, PEG1000, Supporting Information.

mM MgCl$_2$ only 1.2% of the RNA molecules are folded in aqueous solution, but 50% are folded in solutions containing 18% PEG1000. Thus, molecular crowding dramatically shifts the folding equilibrium toward more compact structures under the low Mg^{2+} conditions found *in vivo*.

Lambert and Draper showed that the stabilizing effects of osmolytes and MgCl$_2$ are not additive, and can be antagonistic.[21] Their reasoning was that osmolytes are held close to the RNA surface and thus interfere with the stabilizing

effects of Mg^{2+}, which are also close to the RNA surface. We note that for the crowders investigated in the present work the stabilization is additive with that from MgCl$_2$ and NaCl, at least within the transition regions we investigate. Contrary to the small osmolyte example, we expect that entropic effects drive the stabilization from PEG due to its greater size. It is therefore reasonable that a large crowder would interfere less with close association of Mg^{2+} ions, thus reducing potential antagonism.

Further evidence for the dominance of excluded volume effects is provided by comparison of titrations with EG. Figure S1e (Supporting Information) shows that EG shifts the folding midpoint to lower MgCl$_2$ values, but not as much as PEG. We expect the surface-driven effects of PEG to be significantly smaller than EG due to the lower surface area. Therefore, the stabilization in PEG solutions must be predominantly driven by excluded volume, or entropic, effects.

In NaCl, the stabilization energy due to PEG is smaller in magnitude than in MgCl$_2$, reaching a value of -1.4 ± 0.2 RT (-0.9 ± 0.2 kcal/mol at 37 °C) at 18% PEG1000 (Figure 3b). This observation suggests that either the unfolded or folded states of the RNA (or both) must be qualitatively changed by the presence of PEG, and that this change must rely on the salt cosolute. We believe that the most likely explanation comes due to changes to the unfolded state (Figure 1a), and corresponding differences in the entropy of this state. Since the "unfolded state" is an ensemble of RNA structures that are in equilibrium with the folded state, their thermodynamic state also changes as the salt concentration increases and the folding transition progresses. We therefore attempted to quantify these structural perturbations to the unfolded ensemble using the full scattering functions.

Crowding Orders RNA Chains. To compare the RNA structures in water and PEG solutions, we selected scattering functions that correspond to the same average global structure, as parametrized by R_g. Two such functions are plotted as $QI(Q)$ vs Q in Figure 4a, for RNA folded in MgCl$_2$ and either 1% or 10% PEG8000. In 10% PEG, the scattering is more intense at higher Q-values. Qualitatively, this shows that structural correlations within the RNA at the relevant length scales ($Q > 0.06$ Å^{-1}, $R < 2\pi/Q \approx 100$ Å) are more prevalent. Since these scattering functions were chosen because they represent the same R_g, the normalized $I(Q)$s are, by definition, identical in the Guinier region below $Q = 0.025$ Å^{-1}.

In crowded solutions, we find that higher PEG concentration and larger PEG M_W result in unfolded or intermediate RNA conformations that give higher scattering intensities at $Q > 0.06$ Å^{-1} and are thus more structurally ordered. This indicates that the (primarily) electrostatic stabilization of the folded RNA by ions (MgCl$_2$ and NaCl) is different from the (primarily) entropic stabilization by crowders and leads to a different folding pathway.

The distance distribution functions calculated using GNOM[45] from the scattering functions in Figure 4a are shown in Figure S2a, Supporting Information. This shows that the probability distribution for RNA in the crowded solution is lower in the range 20−70 Å, with this probability being shifted to longer distances. This is in line with an increased repulsion between different domains of the RNA molecules in the crowded solution and therefore higher structural correlation. Shown in Figure 5 are comparisons between the distance distribution functions for selected scattering functions in the 0% and 18% PEG1000 titrations. This shows how PEG compresses the unfolded RNA for a given MgCl$_2$ concen-
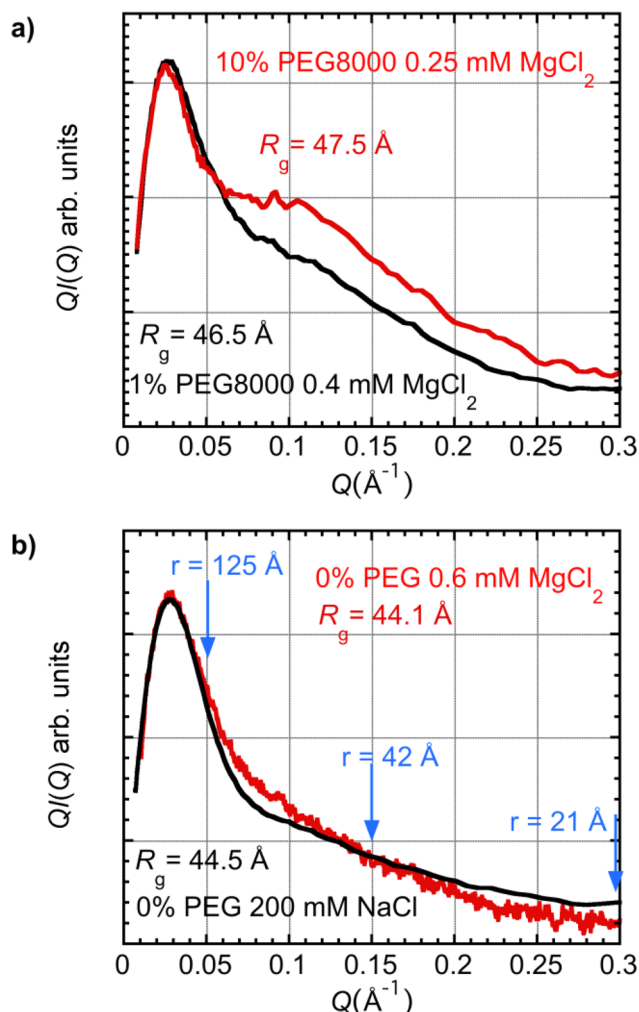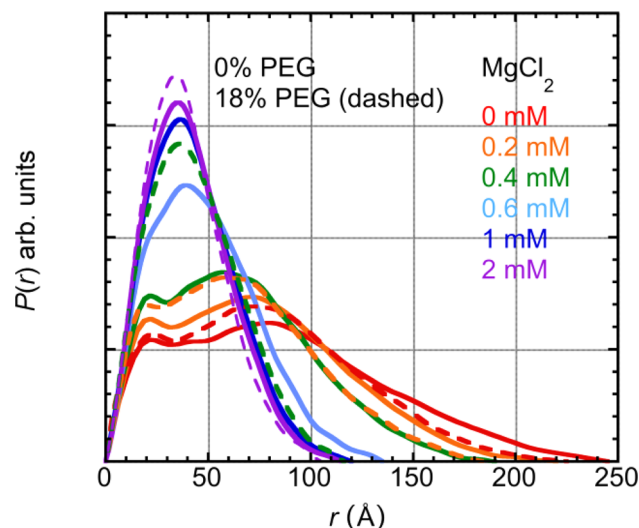
Figure 5. RNA distance distribution functions for RNA in crowded and uncrowded solutions. These probability distribution functions are calculated using GNOM[45] and show how the unfolded RNA at 0 mM $MgCl_2$ is compressed in the crowded solution. These plots represent a selected number of scattering functions in the 0 and 18% PEG1000 titrations.

thus the integral in eq 4 can be evaluated (Rob Rambo, private communication). $2\pi l_c/V$ is plotted as a function of R_g in Figure 6 for RNA in $MgCl_2$ in a series of PEG 8000 solutions.
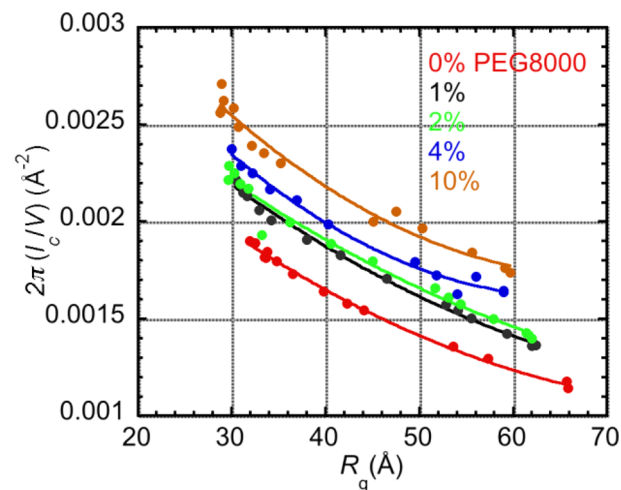

Figure 4. Correlation lengths of folding intermediates. Scattering functions of the *Azoarcus* ribozyme in intermediate folding conditions. Each pair of curves represents samples with the same R_g. The area under the curve yields the correlation length relative to the sample volume, l_c/V. (a) RNA folded in $MgCl_2$ and 1% or 10% PEG8000. The sample of higher ionic strength (0.4 mM $MgCl_2$ black line) has lower scattering intensity above the Guinier region, resulting in a lower integral of $QI(Q)$ and thus lower l_c/V (eq 4). (b) Samples with no crowders folded in $MgCl_2$ (red) or NaCl (black). These data have identical integrals of $QI(Q)$ and thus l_c/V, but systematic differences are observed above the Guinier region. The correlation length is marked in blue for three selected Q-values: $r = 2\pi/Q$.

Figure 6. Molecular crowding increases local structure. The correlation length per scattering volume, l_c/V, of the *Azoarcus* ribozyme plotted as a function of R_g for RNA particles in solutions containing PEG8000 as a macromolecular crowder and $MgCl_2$ as the counterion. l_c/V is calculated according to eq 4 by integrating $QI(Q)$ over the scattering function ($Q = 0$ to ∞ Å^{-1}). The values shown here are calculated with integration limits of $Q = 0.015$ to 0.3 Å^{-1}. Outside this region the scattering functions are identical, see Figure 4 for examples. Thus the absolute values plotted are shifted by an undefined correction term, but the relative order of the values is correct.

tration: compare the functions for 0 mM $MgCl_2$. It also shows that for RNA with similar R_gs in the middle of the transition there are small structural deviations, for example compare the plots at 0.4 and 0.2 mM $MgCl_2$ in 0 and 18% PEG, respectively. A fuller range of distance distribution functions for these titrations are shown in Figure S2b−c, Supporting Information.

The correlation length per scattering volume, l_c/V, of a particle can be calculated using the relation:[46]

$$\int_0^\infty \frac{QI(Q)dQ}{I(0)} = \frac{(\Delta\rho)^2 V \cdot 2\pi l_c}{(\Delta\rho)^2 V^2} = 2\pi\frac{l_c}{V} \quad (4)$$

where $\Delta\rho$ is the electron density difference between particle and solution. This formalism is convenient because, unlike $Q^2I(Q)$ vs Q (Kratky plot), the function $QI(Q)$ converges toward zero at high Q for both folded and unfolded RNA, and

Equivalent plots for RNA in $MgCl_2$ plus PEG 1000 as well as RNA in NaCl plus PEG 1000 and PEG 3350 are shown in Supplemental Figure S3a−d, Supporting Information. Though some of the data presented in these plots have considerable scatter, particularly for the higher % and M_w PEG solutions, as

the RNA folds we observe a decrease in R_g and an increase in $2\pi l_c/V$.

We make two general observations by comparing RNA structures with the same R_g: (1) higher PEG content, and correspondingly lower salt content, results in higher values for l_c/V; (2) without PEG, folding in NaCl or in MgCl$_2$ results in similar l_c/V (Figure S3f, Supporting Information). If we compare scattering functions from the same type of RNA particle with identical R_gs we can assume that the scattering volume V is constant and therefore changes to l_c/V reflect changes to l_c. The correlation length, l_c, can be shown to be equal to the integral of a normalized electron density correlation function over the extent of the particle,[46] or, equivalently, the weight average of a chord distribution that describes how well the particle self-correlates under displacement.

A higher value of l_c thus demonstrates higher intraparticle correlation between segments of the RNA. For particles with identical R_gs, a lower value of l_c/V presumably corresponds to a higher number of alternative structures with the same R_g, or higher flexibility. Using a specific partial volume of 0.508 mL/g for RNA[47] which is only approximate for our samples, we calculate l_c = 10.3 Å and 21.5 Å for *Azoarcus* ribozyme with $2\pi(l_c/V) = 0.0012$ and 0.0025, respectively, corresponding to the extreme folded and unfolded RNAs in Figure 6.

Interpreting l_c as a measure of internal flexibility is in accord with recent single molecule FRET experiments[48] that have shown higher flexibility in a tethered tetraloop-receptor RNA for molecules in higher ionic strength solutions. Further, the authors showed that there is a transition-like increase in this flexibility in the folding transition region, in accord with the salt dependence of the persistence length l_p of stiff polyelectrolytes (see 49 and references therein). A similar effect was observed recently for two DNA duplexes joined by a short polyethylene glycol linker.[50] The number of possible conformational states, and therefore entropy, of this analogue of an unfolded RNA molecule increased with increasing solution ion content.

Flexibility of Unfolded RNA. The shortening of l_c/V as R_g increases reflects the lower order present in the unfolded scattering ensemble compared with the folded RNA ensemble, as well as the general change in particle shape. For example, simulated scattering profiles for a sphere with radius 30 Å give value of $2\pi l_c/V$ of 0.0026 Å^{-2} whereas a cylinder with cross-sectional radius 20 Å and length 90 Å, and therefore the same volume as the sphere, has a value of $2\pi l_c/V$ of 0.0024 Å^{-2}. The values of l_c from these shapes are 46.4 and 42.7 Å for the sphere and the cylinder, respectively. In general, more compact particles with a given V (i.e., closer to a sphere) have higher values of l_c.

We reason that incomplete electrostatic screening, and lower RNA flexibility, in solutions with lower MgCl$_2$ and higher PEG restricts the conformations that the RNA can take due to higher mutual repulsion between sections of the RNA. PEG lowers the R_g by confining the RNA to a smaller volume, but without increasing the local flexibility of the RNA chain. This means that the positions and movements of sections of the RNA influence each other more, and are therefore more strongly correlated. These correlations result in higher scattering beyond the Guinier region. This general principle is clearly moderated by other effects. For example, the condensation of Mg^{2+} ions around the RNA, and thus the local electrostatic potential, will depend on the RNA structure and the presence of other ions and cosolutes.

Mg^{2+} Produces More Ordered Folding Intermediates. Interestingly, we do not observe a difference between l_c/V for RNA structures folded to the same average R_g with MgCl$_2$ and NaCl, although the folding transition occurs at a significantly higher bulk ionic strength in NaCl solutions (see Figure S3f, Supporting Information) for comparisons in uncrowded solutions). Closer inspection, however, reveals some systematic differences between the folding intermediates in Mg^{2+} and Na$^+$. As illustrated in Figure 4b, scattering functions corresponding to R_g = 44 Å in 0.6 mM MgCl$_2$ and 200 mM NaCl, respectively, yield the same integral giving l_c/V. However, the scattering intensity in the region $0.05 \leq Q \leq 0.15$ Å^{-1} is higher in MgCl$_2$, while above $Q = 0.15$, $I(Q)$ is higher in NaCl. Following the above reasoning, this means that the ribozyme samples fewer intraparticle conformations in the $42 - 125$ Å length scales in MgCl$_2$ than in NaCl, leading to greater intraparticle structural correlation and higher scattering intensity. At length scales shorter than 42 Å, however, the opposite is true: the intraparticle correlation is greater in NaCl than MgCl$_2$.

We hypothesize that this reduction in long-range order may be the reason why the stabilizing effect of PEG is greater in solutions containing MgCl$_2$ than it is with NaCl (Figure 3). The reduced long-range order in MgCl$_2$ implies a lower configurational entropy of the ensemble of unfolded states (with a given R_g) in MgCl$_2$ compared with NaCl. This is in line with the observed increase in the entropy of the 'unfolded' state with increasing salt in ref 50. By way of contrast, the scattering intensity in MgCl$_2$ was lower than in NaCl at short length scales comparable to a few nucleotides (below 42 Å, above $Q = 0.15$ Å^{-1}). This is qualitatively consistent with recent persistence length measurements on single stranded RNA molecules. In these measurements, l_p was found to be shorter in MgCl$_2$ solutions compared to NaCl solutions at the same activity corrected ionic strength.[51] Additionally, fits to SAXS data gave lower l_ps for unfolded RNA with comparable R_gs in MgCl$_2$ compared with NaCl.[49]

Recent simulations showed differences between the structures of electrostatically relaxed (but not folded, no tertiary contacts present) RNA molecules in MgCl$_2$ and NaCl.[19] This state was more randomly structured in NaCl than in MgCl$_2$, because in MgCl$_2$ the electrostatically relaxed "unfolded" state was characterized by an increased tendency for the helices to align due to a greater propensity for self-organization of the Mg^{2+} ions.

Thus, this relaxed state, representing the unfolded RNA in the transition region, is characterized by a smaller l_p,[49,51] but more structure,[19] and therefore lower entropy in MgCl$_2$ than in NaCl.[50] The entropy of the folded state, however, is less dependent on the stabilizing salt. It follows therefore that the energy difference between unfolded and folded, $\Delta\Delta G$, is greater with the lower ionic strength of MgCl$_2$ rather than NaCl.

Crowding Changes Entropy Landscape of RNA Folding. The difference in intrachain flexibility indicates that crowders alter the entropy of folding, not only by confining the RNA to a smaller volume, but also by reducing the internal flexibility (and thus entropy) of the unfolded RNA. As illustrated schematically in Figure 7a, the RNA segments are less mobile with respect to each other when folded in low Mg^{2+} and high crowder (orange), than when folded in uncrowded, high salt solutions (red). To put the two scenarios in context, assume that the R_g is 54−55 Å. The RNA on the left corresponds to, for example, RNA stabilized in 0.45 mM MgCl$_2$
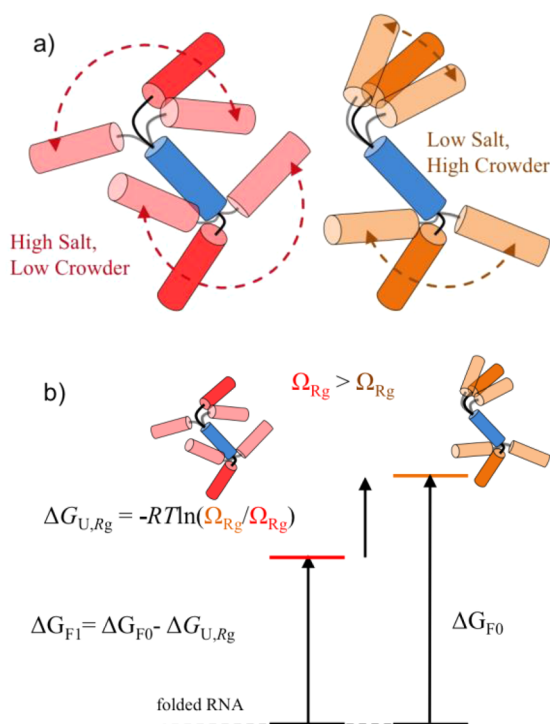
Figure 7. Molecular crowding changes the RNA folding landscape. (a) Schematic illustration of a central RNA double helix (blue cylinder) connected by single stranded sections (black/gray lines) to helical "arms" (orange, low salt, high crowder; red, high salt, low crowder). The two arms make the same contributions to the RNA's radius of gyration, so that R_g (low salt, left) = R_g (high salt, right). Due to the higher flexibility of the arms in high salt, the number of conformations, Ω, is greater, raising the entropy of the unfolded state. (b) Energy level diagram illustrating the change in folding energy differences ΔG_F due to changes to the unfolded state's flexibility. On the right is the baseline folding free energy ΔG_{F0}. The unfolded RNA on the left (red) has greater flexibility and therefore higher configurational entropy than the unfolded state on the right (orange). $G_U - G_U = \Delta G_{U,R_g} = -RT \ln(\Omega_{R_g}/\Omega_{R_g})$, where $\Omega_{R_g} > \Omega_{R_g}$ so ΔG is positive, correctly identifying the higher entropy (red) state as the lower energy state. Thus, ΔG_{F1} is smaller than ΔG_{F0}.

and 0% PEG (red data point at 54 Å in Figure 6). The RNA on the right corresponds to RNA stabilized in 0.1 mM $MgCl_2$ and 10% PEG8000 (orange data point at 55 Å in Figure 6). We suggest this means that a smaller fraction of the energy landscape is accessible to RNA in the crowded solution due to the lower concentration of Mg^{2+} ions restricting its local mobility.

A second possible contribution to restricted local mobility in crowded solutions is simple steric interference of the crowders themselves. The PEG molecules are chain-like and so it is possible that part of them can reside within the volume that is swept out by the unfolded RNA, at least temporarily. This will necessarily restrict the conformations that the unfolded RNA can adopt and most probably will preferentially shift the occupation of U states to those with highest $R_{g,U}$. Hypothetically then, the steric interference of crowders can have two effects that act in opposite directions on global R_g: (1) the U state is pushed into more expanded conformations, increasing R_g; (2) restricting conformations of U reduces that ensemble's entropic weight thus stabilizing the folded state, and decreasing observed R_g. Our data do not allow us to extract the balance of

the competing effects. The lowering of the entropy of U due to steric restriction, however, leads to higher values of l_c/V in the crowded solution.

Figure 7b illustrates the effect that lower flexibility for unfolded RNA has on the folding energy levels. We assume that differences between the folded RNA structure in crowded and dilute solutions are negligible in comparison with those differences between the unfolded RNA structures in crowded and dilute solutions. This can be rationalized by the smaller reduction in the volume occupied by the folded RNA in crowded solutions, and by tertiary interactions that restrict its conformational space. Following the color code from Figure 7a, there is a larger energy gap between the less flexible unfolded RNA and the folded state. This is a general result and does not depend on the physical origin of the change in flexibility. We anticipate therefore that the lower flexibility (lower entropy) of the unfolded ensemble in crowded solutions contributes to the increase in ΔG_F and therefore adds to the folded state stability.

Additionally, we postulated above that the lower $\Delta\Delta G$ in NaCl than in $MgCl_2$ was due to increased order of the unfolded RNA in $MgCl_2$. In Figure 7b, this would manifest itself as a smaller change in folding energy due to PEG, $\Delta G_{U,R_g}$, in the NaCl solutions, because the unfolded RNA loses less entropy due to their generally higher ionic strength. PEG may also decrease the entropy of the folded state in NaCl, much more than in $MgCl_2$, further reducing $\Delta\Delta G$ in NaCl. This is because the folded state is more dynamic in NaCl than in $MgCl_2$, based on its slightly greater R_g in NaCl and weaker protection of the RNA backbone in footprinting experiments.[52] We conclude that molecular crowding can reshape RNA folding energy landscapes by altering the average structures of the unfolded and partially folded RNAs.

■ ASSOCIATED CONTENT

Ⓢ Supporting Information

Plots of MgCl and NaCl titrations, correlation lengths and tables of fit parameters. This material is available free of charge via the Internet at http://pubs.acs.org.

■ AUTHOR INFORMATION

Corresponding Author

rbriber@jhu.edu; swoodson@jhu.edu

Present Address

J.H.R.: Code 6120, Chemistry Division, Naval Research Laboratory, Washington, DC 20375. R.B.: Department of Cell Biology, Harvard Medical School, 240 Longwood Ave, LHRBB 520, Boston MA 02115

Notes

The authors declare no competing financial interest.

■ REFERENCES

(1) Doudna, J. A.; Cech, T. R. *Nature* **2002**, *418*, 222.

(2) Ellis, R. J. *Trends Biochem. Sci.* **2001**, *26*, 597.

(3) Zhou, H.-X.; Rivas, G.; Minton, A. P. *Ann. Rev. Biophys.* **2008**, *37*, 375.

(4) Manning, G. S. *Q. Rev. Biophys.* **1978**, *11*, 179.

(5) Misra, V. K.; Draper, D. E. *J. Mol. Biol.* **2000**, *299*, 813.

(6) Draper, D. E.; Grilley, D.; Soto, A. M. *Annu. Rev. Biomol. Struct.* **2005**, *34*, 221.

(7) Cheatham, T. E. *Curr. Opin. Struct. Biol.* **2004**, *14*, 360.

(8) Thirumalai, D.; Klimov, D. K.; Lorimer, G. H. *Proc. Natl. Acad. Sci.* **2003**, *100*, 11195.

(9) Minton, A. P. *Biopolymers* **1981**, *20*, 2093.

(10) Minton, A. P. *Methods Enzym.* **1998**, *295*, 127.

(11) Minton, A. P. *Curr. Opin. Struc. Biol.* **2000**, *10*, 34.

(12) Minton, A. P. *Biophys. J.* **2000**, *78*, 101.

(13) Zhou, H.-X.; Qin, S. *Phys. Rev. E* **2010**, *81*, 031919.

(14) Rubinstein, M.; Colby, R. H. *Polymer Physics*; Oxford University Press: Oxford, 2003.

(15) Nashimoto, M. *Eur. J. Biochem.* **2000**, *267*, 2738.

(16) Nakano, S.; Karimata, H. T.; Kitagawa, Y.; Sugimoto, N. *J. Am. Chem. Soc.* **2009**, *131*, 16881.

(17) Nakano, S.-I.; Kitigawa, Y.; Karimata, H. T.; Sugimoto, N. *Nucleic Acids Symp.* **2008**, *52*, 519.

(18) Denesyuk, N. A.; Thirumalai, D. *J. Am. Chem. Soc.* **2011**, *133*, 11858.

(19) Tan, Z.-J.; Chen, S.-J. *Biophys. J.* **2012**, *103*, 827.

(20) Hong, J.; Gierasch, L. M. *J. Am. Chem. Soc.* **2010**, *132*, 10445.

(21) Lambert, D.; Draper, D. E. *J. Mol. Biol.* **2007**, *370*, 993.

(22) Miklos, A. C.; Sarkar, M.; Wang, Y.; Pielak, G. J. *J. Am. Chem. Soc.* **2011**, *133*, 7116.

(23) Ignatova, Z.; Krishnan, B.; Bombardier, J. P.; Marcelino, A. M. C.; Hong, J.; Gierasch, L. M. *Peptide Sci.* **2007**, *88*, 157.

(24) Kilburn, D.; Roh, J. H.; Guo, L.; Briber, R. M.; Woodson, S. A. *J. Am. Chem. Soc.* **2010**, *132*, 8690.

(25) Chauhan, S.; Caliskan, G.; Briber, R. M.; Perez-Salas, U. A.; Rangan, P.; Thirumalai, D.; Woodson, S. A. *J. Mol. Biol.* **2005**, *353*, 1199.

(26) Rangan, P.; Masquida, B.; Westhof, E.; Woodson, S. A. *Proc. Natl. Acad. Sci.* **2003**, *100*, 1574.

(27) Silverman, S. K.; Cech, T. R. *Biochemistry* **1999**, *38*, 8691.

(28) Baird, N. J.; Westhof, E.; Qin, H.; Pan, T.; Sosnick, T. R. *J. Mol. Biol.* **2005**, *352*, 712.

(29) Fang, X.; Pan, T.; Sosnick, T. R. *Biochemistry* **1999**, *38*, 16840.

(30) Kuznetsov, S. V.; Shen, Y.; Benight, A. S.; Ansari, A. *Biophys. J.* **2001**, *81*, 2864.

(31) Ma, H.; Proctor, D.; Bevilacqua, P.; Gruebele, M. *J. Am. Chem. Soc.* **2006**, *128*, 1523.

(32) Chauhan, S.; Woodson, S. A. *J. Am. Chem. Soc.* **2008**, *130*, 1296.

(33) Moghaddam, S.; Caliskan, G.; Chauhan, S.; Hyeon, C.; Briber, R. M.; Thirumalai, D.; Woodson, S. A. *J. Mol. Biol.* **2009**, *393*, 753.

(34) Draper, D. E. *Biophys. J.* **2008**, *95*, 5489.

(35) Record, M. T., Jr.; Anderson, C. F.; Lohman, T. M. *Q. Rev. Biophys.* **1978**, *11*, 103.

(36) Tan, Z.-J.; Chen, S.-J. *Biophys. J.* **2006**, *90*, 1175.

(37) Leipply, D.; Draper, D. E. *Biochemistry* **2010**, *49*, 1843.

(38) Cohen, J. A.; Podgornik, P. R.; Hansen, P. L.; Parsegian, V. A. *J. Phys. Chem. B* **2009**, *113*, 3709.

(39) Briber, R. M.; Liu, X.; Bauer, B. J. *Science* **1995**, *268*, 395.

(40) Nakano, S.; Karimata, H.; Ohmichi, T.; Kawakami, J.; Sugimoto, N. *J. Am. Chem. Soc.* **2004**, *126*, 14330.

(41) Miyoshi, D.; Karimata, H.; Sugimoto, N. *J. Am. Chem. Soc.* **2006**, *128*, 7957.

(42) Muhuri, S.; Mimura, K.; Miyoshi, D.; Sugimoto, N. *J. Am. Chem. Soc.* **2009**, *131*, 9268.

(43) Roh, J. H.; Guo, L.; Kilburn, J. D.; Briber, R. M.; Irving, T.; Woodson, S. A. *J. Am. Chem. Soc.* **2010**, *132*, 10148.

(44) Knowles, D. B.; LaCroix, A. S; Deines, N. F.; Shkel, I.; Record, M. T., Jr. *Proc. Natl. Acad. Sci.* **2011**, *108* (31), 12699.

(45) Svergun, D. *J. Appl. Crystallogr.* **1992**, *25*, 495.

(46) Porod, G. General Theory. In *Small Angle X-ray Scattering*; Glatter, O., Kratky, O., Eds.; Academic Press: London, 1982; pp 18–51.

(47) Bonifacio, G. F.; Brown, T.; Conn, G. L.; Lane, A. N. *Biophys. J.* **1997**, *73*, 1532.

(48) Fiore, J. L.; Hodak, J. H.; Piestert, O.; Downey, C. D.; Nesbitt, D. J. *Biophys. J.* **2008**, *95*, 3892.

(49) Caliskan, G.; Hyeon, C.; Perez-Salas, U.; Briber, R. M.; Woodson, S. A.; Thirumalai, D. *Phys. Rev. Lett.* **2005**, *95*, 268303.

(50) Bai, Y.; Chu, V. B.; Lipfert, J.; Pande, V. S.; Herschlag, D.; Doniach, S. *J. Am. Chem. Soc.* **2008**, *130*, 12334.

(51) Chen, H.; Meisburger, S. P.; Pabit, S. A.; Sutton, J. L.; Webb, W. W.; Pollack, L. *Proc. Natl. Acad. Sci.* **2012**, *109*, 799.

(52) Rangan, P.; Woodson, S. A. *J. Mol. Biol.* **2003**, *329*, 229.